Carcinogenesis vol.33 no.6 pp.1231–1238, 2012
doi:10.1093/carcin/bgs137
Advance Access publication March 29, 2012

Gut microbiota accelerate tumor growth via c-jun and STAT3 phosphorylation in APC$^{Min/+}$ mice

Yinghui Li[1,2], Parag Kundu[1,3], Shih Wee Seow[4], Cristina Teixeira de Matos[1], Linda Aronsson[1], Keh Chuang Chin[2], Klas Kärre[1], Sven Pettersson[1,3,4,*] and Gediminas Greicius[4]

[1]Department of Microbiology, Tumor and Cell Biology (MTC), Karolinska Institutet, Stockholm 117 77, Sweden, [2]Singapore Immunology Network (SIgN), A*STAR, 8A Biomedical Grove, Singapore 138648, [3]School of Biological Sciences, Nanyang Technological University, 60 Nanyang Drive, Singapore 637551, Singapore and [4]National Cancer Centre, 11 Hospital Drive, Singapore 169610, Singapore

*To whom correspondence should be addressed. Tel: +46 8 5248 6686; Fax: +46 8 33 15 47
Email: sven.pettersson@ki.se

Chronic inflammation is increasingly recognized as a major contributor of human colorectal cancer (CRC). While gut microbiota can trigger inflammation in the intestinal tract, the precise signaling pathways through which host cells respond to inflammatory bacterial stimulation are unclear. Here, we show that gut microbiota enhances intestinal tumor load in the APC$^{Min/+}$ mouse model of CRC. Furthermore, systemic anemia occurs coincident with rapid tumor growth, suggesting a role for intestinal barrier damage and erythropoiesis-stimulating mitogens. Short-term stimulation assays of murine colonic tumor cells reveal that lipopolysaccharide, a microbial cell wall component, can accelerate cell growth via a c-Jun/JNK activation pathway. Colonic tumors are also infiltrated by CD11b+ myeloid cells expressing high levels of phospho-STAT3 (p-Tyr705). Our results implicate the role of gut microbiota, through triggering the c-Jun/JNK and STAT3 signaling pathways in combination with anemia, in the acceleration of tumor growth in APC$^{Min/+}$ mice.

Introduction

Chronic inflammation and colon cancer progression are irrefutably linked in inflammatory bowel disease patients since cancer susceptibility correlates with the extent and duration of colonic disease/mucosal inflammation. Accumulating evidence demonstrate that inflammatory cells in the tumor microenvironment and their products can enhance progression of cancer in conjunction with the supporting stromal cells. Moreover, inflammatory cells secrete a variety of pro-inflammatory molecules and growth factors that can stimulate tumor cell proliferation, survival, migration, apoptosis and angiogenesis (1). Notably, cytokines like interleukin (IL)-6 (2) and IL-23 (3) as well as factors acting downstream of the activation cascade of the transcription factor (TCF) nuclear factor-kappaB (NF-κB) have been implicated to play an important role in cancer development and dissemination (4).

Interestingly, NF-κB activation can result from components of gut microflora. Enteric microflora play a pivotal role in gut inflammation as demonstrated by the efficacy of antibiotics in ameliorating the severity of inflammation in inflammatory bowel disease patients (5). Furthermore, many animal models of colitis show that the intestinal inflammation and presence of invading inflammatory cells are abrogated when the animals are derived into germ-free (GF) environment, i.e. an environment devoid of microbiota (6).

The APC$^{Min/+}$ mice carry a mutation in the tumor suppressor gene, adenomatous polyposis coli (APC) and demonstrate a consequent predisposition to multiple intestinal neoplasia (Min) (7). This mutation leads to aberrant activation of the Wnt/β-catenin signaling pathway in the colonic epithelium (8). This activation, however, requires additional signaling components that synergistically push the aberrant epithelial cell into accelerated cell growth. Two such cofactors have been described. While phosphorylation of the activator protein 1 (AP-1) TCF c-Jun can promote intestinal tumor growth in APC$^{Min/+}$ mice through interaction with TCF-4 in a β-catenin-dependent fashion (9), phosphorylation of the TCF STAT3 has been connected to the increased tumor invasion and poorer prognosis of human colorectal adenocarcinoma (10).

In human colorectal cancers (CRCs) as well as in animal models of CRC, the compromised intestinal epithelial lining elicits severe inflammation frequently connected with bleeding and anemia. Common treatment regimes are to restore the levels of erythrocytes by use of erythropoietin (EPO). Although EPO is documented for its capacity to restore hemoglobin levels (11), its efficacy in correcting anemia in patients with advanced colorectal tumor growth is still controversial. This is in part due to the observation that EPO receptor expression is detectable in tumor tissues indicating that EPO-R expression is not restricted to erythrocytes alone.

Here we report that specific pathogen-free (SPF) APC$^{Min/+}$ mice, when derived into GF conditions, display a drastic drop in colonic tumor incidence as well as reduced overall tumor load. In contrast, SPF APC$^{Min/+}$ mice exhibit high tumor load, splenomegaly and anemia with a massive infiltration of inflammatory cells arising from a dysfunctional intestinal epithelial barrier at advanced ages. Moreover, colonic tumors from these mice display elevated levels of phosphorylated c-Jun and STAT3 (p-Tyr705), with infiltrating CD11b+ myeloid cells expressing nuclear p-STAT3 (Tyr-705).

Abbreviations: AP-1, activator protein 1; APC, adenomatous polyposis coli; CRC, colorectal cancer; EPO, erythropoietin; FITC, fluorescein isothiocyanate; GF, germ free; IL, interleukin; LPS, lipopolysaccharide; mRNA, messenger RNA; SPF, specific pathogen free; TCF, transcription factors.

Materials and methods

Animals and study design

The colony of C57BL/6J-APC$^{Min/+}$ mice was maintained under SPF or (GF) environment at the Center For Gnotobiotic Research (CFGR), Karolinska Institutet. The studies were performed in agreement with Swedish ethical regulations. Murine EPO (BD Pharmingen) was administered for 7 days as daily intraperitoneal injections at the dose of 1000 U/kg. Control group of mice received injections of sterile phosphate-buffered saline (PBS). Mice were killed after either 1 day or 21 days following EPO treatment (Supplementary Figure S9A is available at *Carcinogenesis* Online). Sets of at least six age- and gender-matched mice were used in each single experiment with EPO treatment. For tumor counting, the whole intestine was fixed in PBS-buffered 4% formalin solution and cut longitudinally. Only clearly defined adenomas exceeding 0.8 mm, under dissection microscope, were counted as tumors.

Immunohistochemistry

Colonic tissue from APC$^{Min/+}$ mice was fixed in 4% formaldehyde, cryopreserved in 20% sucrose and sectioned on a cryostat. In order to visualize p-STAT3 (Tyr-705) staining, sections were blocked in 10% donkey serum (Jackson Laboratory) in PBS containing 0.05% Tween20 for 45 min and then incubated overnight at 4°C using rabbit monoclonal p-STAT3 (Tyr-705) antibody (Cell Signaling) or control immunoglobulin G at 1:100 dilution. The slides were then washed in PBS containing 0.05% Tween20 and incubated with Alexa Fluor 594 anti-rabbit secondary antibody (Invitrogen). 4′,6-Diamidino-2-phenylindole was used for nuclear staining.

Western blot analysis

Samples for western blot were prepared as follows: intestine was washed in ice-cold PBS and then cut longitudinally. Adenomas were cut out, placed into lysis buffer (20 mM Tris pH 7.5, 150 mM NaCl, 1 mM ethylenediaminetetraacetic acid, 1% Triton X, 1 mM dithiothreitol) supplemented with complete ethylenediaminetetraacetic acid-free protease inhibitor (Roche) and phosphatase inhibitors (5 mM sodium fluoride and 0.4 mM sodium vanadate) before being disintegrated using sterile scissors. Intestinal mucosa was gently scraped using scalpel, homogenized and then lysed. Samples were analyzed using

sodium dodecyl sulfate gel electrophoresis and western blotting, using 50 μg of protein extracts per lane. Polyvinylidene difluoride membranes were incubated with anti-STAT3, anti-p-STAT3 (Tyr-705) (Cell Signaling), anti-p-cjun (Ser63/73) or anti-β-actin (Santa Cruz Biotechnology) antibodies and then incubated with peroxidase-conjugated secondary antibodies (Dako). To assay STAT3 activation in curcumin-treated tumors, $APC^{Min/+}$ mice with fecal occult blood were treated with curcumin (Sigma) by oral gavage for 5 days at a dose of 100 mg/kg. Control group of mice received sterile PBS. After harvesting, samples were processed for western blotting as outlined above.

Real-time quantitative PCR

Total RNA was extracted from purified splenic CD11b+ cells and mouse intestinal tissues using PicoPure RNA isolation kit (Arcturus) and RNeasy RNA isolation kit (Qiagen), respectively, according to manufacturers' instructions. Complementary DNA synthesis was performed using Superscript II (Invitrogen). The following mouse primer sequences were used for real-time PCR quantification: tumor necrosis factor-α forward—5′-CAAATGGCCTCCCTCTCAT-3′ and reverse—5′-CTCCTCCACTTGGTGGTTTG-3′; IL-1β forward—5′-GCTGAAAGCTCTCCACCTCA-3′ and reverse—5′-GGCCACAGGTATTTTGTCGT-3′; IL-23 (p19) forward—5′-GCACCTGCTTGACTCTGACA-3′ and reverse—5′-ATCCTCTGGCTGGAGGAGTT-3′; Bcl-3 forward—5′-GAGTCCTCCGAGGCCCTGGCCGGCCCGTAC-3′ and reverse—5′- AATAATTTACACTGTGATCAATGCCCTCCC-3′ and β-actin forward—5′ CTGTATTCCCCTCCATCGTG-3′ and reverse—5′-CCTCGTCACCCACATAGGAG-3′. Quantitative real-time PCR was performed in triplicates for each sample on an ABI 7500 Real-time PCR System (Applied Biosystems) using Power SYBR Green PCR Mastermix (Applied Biosystems). Data are presented as fold change of relative gene expression.

Fluorescein isothiocyanate-dextran assay

$APC^{Min/+}$ ($n = 5$) and B6 mice ($n = 6$) were administered with 4.4 mg of fluorescein isothiocyanate (FITC)-labeled dextran (molecular weight 4000; Sigma) in PBS via oral gavage. After 2 h and 40 min, blood samples were collected by cardiac puncture and measured for fluorescence using a FITC filter set in TECAN Infinite F200.

Flow cytometry

To remove erythrocytes, splenocyte suspension was lysed in erythrocyte lysis buffer, washed and counted. Bone marrow cells were prepared from femur and tibia, washed in PBS and counted. Cells (0.5×10^6) were used for each staining group. Cells were blocked in 10% mouse serum for 30 min before incubation with primary antibodies to GR1 (eBiosciences), Ter-119 (BD Pharmingen) and CD11b (AbD Serotec) molecules (diluted 1:100 in PBS/2% mouse serum) for 1 h. Thereafter, cells were washed and incubated with PBS/2% mouse serum containing streptavidin-Alexa-488 (Invitrogen) and anti-c-kit-PE (BD Pharmingen) for 30 min prior to fluorescence-activated cell sorting analysis.

Purification of splenic macrophages

Spleens of $APC^{Min/+}$ mice were dissociated into single cell suspensions, passed through cell strainers (45 μm; Becton Dickinson) and counted. Thereafter, cells were incubated in ice-cold PBS containing CD11b-specific MicroBeads (Miltenyi Biotec GmbH) and 5 mM ethylenediaminetetraacetic acid to reduce cell aggregation. Incubation was performed for 30 min at 4°C. Cell purification was performed using mass spectrometry separation columns according to producer's recommendations. Fluorescence-activated cell sorting analysis of the CD11b+ cells was also performed after mass spectrometry separation columns column separation to check the purity of macrophages (Supplementary Figure S11 is available at *Carcinogenesis* Online). The purified CD11b+ cells were then cultured in RPMI-1640 medium supplemented with 1% fetal bovine serum and penicillin-streptomycin and stimulated with EPO (600 U/ml) for 1 h.

Primary culture of colonic epithelial cells and colonic tumors

Colons from wild-type mice were resected and placed in Dulbecco's modified Eagle's medium (high glucose) supplemented with 1% fetal bovine serum, L-glutamine and penicillin–streptomycin. After cutting the colon into short segments, the tissues were washed and digested at 37°C for 90 min with Dispase I (1 mg/ml) (Roche Diagnostics). The digested mucosa was then flushed gently several times with Dulbecco's modified Eagle's medium to release cells and crypts loosely attached after enzymatic digestion. Subsequently, the cells were plated in 24-well plates (~1.5×10^6 cells per well) coated with a 1:1 solution of Dulbecco's modified Eagle's medium: Matrigel (Becton Dickinson) and allowed to settle for 30 min. Freshly isolated tumor specimens were minced with sterile scissors and processed as per the colonic epithelial cells. Viability of colonic epithelial and tumor cells was routinely >90%. *Ex vivo* cultures were stimulated with lipopolysaccharide (LPS) (5 μg/ml) or EPO (600 U/ml) for the indicated time.

In vitro *stimulation assays*

Mouse colonic carcinoma cell line CT26 was obtained from American Cell Type Culture Collection (ATCC-CRL-2638). Prior to stimulation, cells were starved on serum-free RPMI-1640 medium overnight. Thereafter, cells were stimulated with LPS (5 μg/ml) and/or murine EPO (100 U/ml) for the indicated time. Cell lysates were then prepared and analyzed using western blot.

3-(4,5-dimethylthiazol-2-yl)-5-(3-carboxymethoxyphenyl)-2-(4-sulfophenyl)-2H-tetrazolium proliferation assay

CT26 cells were starved overnight in serum-free medium and then cultured in RPMI-1640 medium containing 0.1% fetal calf serum and the indicated treatments, in the presence and absence of c-Jun kinase inhibitor II (10 μg/ml) for 3 days. Proliferation was measured using AQueousOne proliferation assay (*3-(4,5-dimethylthiazol-2-yl)-5-(3-carboxymethoxyphenyl)-2-(4-sulfophenyl)-2H-tetrazolium*, G3581; Promega). Fifty microliters of AQueousOne reagent was added per well of 500 μl of cell culture medium and incubated until color development (20–30 min). Thereafter, cell culture supernatants were transferred into flat bottom 96-well plates and measured for absorbance at 490 nm using Tecan Infinite F200. The extent of proliferation was determined according to the formula (OD1 − OD2)/OD2, where OD1 is optical density of the test group and OD2 optical density is the 'c-Jun kinase inhibitor II - only treated' group.

Results

GF $APC^{Min/+}$ mice display reduced tumor load

In our initial screen of $APC^{Min/+}$ mice, we found that $APC^{Min/+}$ mice at 8–10 weeks age displayed multiple tumors only in the small intestine. In contrast, $APC^{Min/+}$ mice at 18–25 weeks age developed colonic tumors and showed symptoms of rectal bleeding and anemia that resulted in the expansion of erythroid progenitor cells (Ter119+) in bone marrow and spleen (Supplementary Figure S1 is available at *Carcinogenesis* Online; Figure 3A). As gut microbiota have been suggested to perpetuate inflammation and thus tumor growth (12), we derived SPF $APC^{Min/+}$ mice into GF conditions and monitored their tumor load. We found that GF $APC^{Min/+}$ mice had a significant reduction ($P < 0.05$, Wilcoxon rank-sum test) in intestinal tumor load (Figure 1), demonstrating the pathogenic role of commensal bacteria in tumorigenesis. Moreover, in SPF $APC^{Min/+}$ mice, the mucosal barrier damage resulting from outgrowth of colonic tumors into the intestinal lumen may facilitate translocation of gut microflora into the intestinal lamina propria, thus triggering inflammation and myeloid cell recruitment (Supplementary Figure S4 is available at *Carcinogenesis* Online). Interestingly, a MyD88-dependent mechanism for enhanced regenerative responses to epithelial injury, through activation of NF-κB has been proposed (13). We therefore backcrossed $APC^{Min/+}$ mice with mice carrying a myeloid-specific deletion in IκB kinase β. Our data revealed a significant drop in the tumor load of SPF $APC^{Min/+}$ mice lacking IκB kinase β in myeloid cells (Supplementary Figure S5 is available at *Carcinogenesis* Online), suggesting that a MyD88-dependent activation of NF-κB in myeloid cells, by signals from

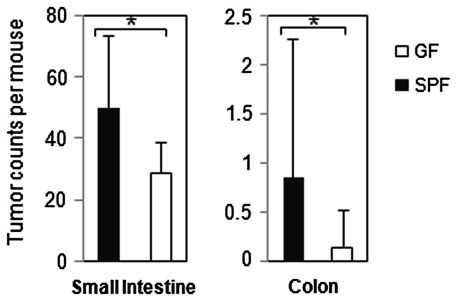

Fig. 1. $APC^{Min/+}$ tumor load is regulated by the presence of intestinal microflora. Tumor growth is reduced in GF $APC^{Min/+}$ mice. Tumor load in small intestine and colon was assessed in SPF and GF mice at 10–17 weeks of age ($n = 27$ and $n = 12$ for small intestine tumor counts, $n = 32$ and $n = 19$ for colon tumor counts, respectively). Error bars represent standard deviation. Significance level of $P < 0.05$ (Wilcoxon rank-sum test) is indicated by an asterisk.

the gut microflora and injured epithelium, can contribute to accelerated colonic tumor growth in $APC^{Min/+}$ mice.

Colonic tumors display an inflammatory profile

Subsequent histological analyses of intestinal tumors from $APC^{Min/+}$ mice revealed that colonic tumors had compromised epithelial-lining integrity, as shown by the discontinuous epithelial lining (marked by arrows in Figure 2A; Supplementary Figure S2 is available at *Carcinogenesis* Online). Moreover, when we assessed mucosal barrier function via FITC-dextran assay, intestinal permeability in 18- to 25-week-old $APC^{Min/+}$ mice was significantly increased ($P < 0.01$, Wilcoxon rank-sum test) as compared with age-matched B6 mice (Figure 2A, right plot). To assess the inflammatory status of intestinal tumors, we analyzed tumor and surrounding normal tissues for recruitment of myeloid cells as well as lymphocytes by immunohistochemistry. We found significantly elevated numbers of CD11b+ and GR1+ cells in colonic tumors than small intestinal tumors, but no significant differences between them in counts of infiltrating T and B lymphocytes (Supplementary Figures S3 and S4 are available at *Carcinogenesis* Online). NK cells were rarely detected in both tumor and mucosal tissues.

Complementary cytokine expression profiling (quantitative real-time–PCR) revealed significantly higher ($P < 0.05$, analysis of variance) messenger RNA (mRNA) levels of tumor necrosis factor α, IL-1β and IL-23 (p19) in colonic tumors of $APC^{Min/+}$ mice, relative to small intestinal tumors as well as normal intestinal mucosa (Figure 2B; Supplementary Figure S6C is available at *Carcinogenesis* Online). Moreover, increased amounts of the biologically active form of IL-1β were detected in colonic tumors, distinct from other tissues (Supplementary Figure S6A is available at *Carcinogenesis* Online). In contrast, expression analysis of T lymphocyte-polarizing cytokines, IL-10 and IL-12A, showed no significant differences between colonic tumors and small intestinal tumors as well as normal mucosa (Supplementary Figure S6B is available at *Carcinogenesis* Online). These findings demonstrate a high inflammatory status in colonic tumors of $APC^{Min/+}$ mice, marked by an enrichment of myeloid cells and increased production of inflammatory cytokines.

Chronic inflammatory circuits are intimately connected with cellular stress-signaling regulators such as the AP-1 and STAT TCFs. To assess whether chronic inflammatory signaling pathways were activated in $APC^{Min/+}$ tumors, we looked for the potential activation of c-Jun and STAT3. Protein analysis of tumors from $APC^{Min/+}$ mice, via densitometry analysis of western blots, revealed significantly higher levels of phosphorylated c-Jun in colonic tumors, as compared with small intestinal tumors (Figure 2C). As AP-1 TCFs have been reported to interact with STAT3 and enhance its transactivation potential (14), we thus examined the phosphorylation status of STAT3 in colonic tumors. Intriguingly, we found significantly elevated levels of phosphorylated STAT3 (p-Tyr705) in $APC^{Min/+}$ colonic tumors as compared with small intestinal tumors and normal intestinal mucosa (Figure 2D). We then probed further to identify the STAT3-activated cell type in colonic tumors and were fascinated to find that majority of cells with nuclear translocation of p-STAT3 (Tyr-705) expressed the myeloid surface marker, CD11b (Figure 2E; Supplementary Figure S7 is available at *Carcinogenesis* Online). These data thus demonstrate a distinct inflammatory status in $APC^{Min/+}$ colonic tumors that correlate with c-Jun and STAT3 activation. In particular, tumor-associated CD11b+ myeloid cells may be the key mediators of colon tumorigenesis via the JAK/STAT3 signaling pathway.

Development of colonic tumors in $APC^{Min/+}$ mice correlates with anemia and expansion of hematopoietic cells

Advanced stages of CRC are frequently associated with anemia due to chronic gastrointestinal bleeding (7,15,16) Consistent with this, $APC^{Min/+}$ mice with advanced tumor load exhibited rectal bleeding, low hematocrit and hemoglobin counts (Supplementary Figure S8 is available at *Carcinogenesis* Online). To assess hematopoietic changes due to anemia, fluorescence-activated cell sorting analysis of bone marrow cells and splenocytes from $APC^{Min/+}$ and wild-type ($APC^{+/+}$) mice were performed. Our analysis revealed an expansion of cells belonging to two major lineages—erythroid cells (Ter119+) and myeloid cells (CD11b-GR1+, CD11b+GR1+) as well as B lymphocytes and NK cells (Figure 3A and B).

EPO treatment of $APC^{Min/+}$ mice elevates tumor load in colon

Having observed that $APC^{Min/+}$ mice, with colonic tumors, displayed anemia and increased p-STAT3 (Tyr-705), we hypothesized that anemia-triggered signaling pathways could promote tumor cell growth. For this purpose, we took advantage of EPO, a hormone known to stimulate proliferation of both myeloid and erythroid cells (17); 8- to 10-week-old $APC^{Min/+}$ mice (without anemia) were injected with EPO or with PBS as a control (Supplementary Figure S9A is available at *Carcinogenesis* Online). After 21 days, animals were killed and analyzed for tumor load. When we scored for tumor load in the colon, a significant increase ($P < 0.05$, Wilcoxon rank-sum test) was observed in the EPO-treated group compared with the PBS-treated group (Figure 4). In contrast, no increase in the tumor load of small intestine was observed (Figure 4). Interestingly, when EPO was administered to GF $APC^{Min/+}$ mice under similar conditions, no acceleration of tumors in colon was observed (one of eight mice developed colonic tumors). Thus, exposure of $APC^{Min/+}$ mice to EPO accelerates tumor growth in the colon in a microflora-dependent manner, without affecting tumors of the small intestine. The EPO-treated group also showed an increase of infiltrating CD11b+ myeloid cells in colonic tumor regions (Supplementary Figure S9B is available at *Carcinogenesis* Online) and increased numbers of mature (c-Kit-) CD11b+ cells in the splenic compartment of $APC^{Min/+}$ mice (Supplementary Figure S9C is available at *Carcinogenesis* Online).

EPO induces STAT3 phosphorylation in CD11b+ myeloid cells of $APC^{Min/+}$ mice

Having observed activated STAT3 in CD11b+ cells infiltrating colonic tumors from $APC^{Min/+}$ mice and in view of earlier work depicting an EPO-induced STAT3 phosphorylation in erythroid cells (18), we further probed whether EPO can modulate STAT3 phosphorylation levels in colonic tumors of $APC^{Min/+}$ mice. Colonic tumors isolated from $APC^{Min/+}$ mice were cultured *ex vivo* and exposed to EPO, in the presence or absence of LPS. After 2 h, extracts were prepared and subjected to western blot analysis of phosphorylated STAT3. Intriguingly, *ex vivo* cultured colonic tumors showed increased p-STAT3 (Tyr-705) following EPO exposure (Figure 5A, lane 2). In contrast, this induction was absent in small intestinal tumors (Figure 5B, lane 5). Having observed elevated levels of activated STAT3 in CD11b+ myeloid cells infiltrating colonic tumors, we next examined whether EPO could influence STAT3 activation in these cells. Anemic $APC^{Min/+}$ mice display a systemic activation of the immune system, including high numbers of CD11b+ cells in the spleen (Figure 3B). Due to limitations in obtaining sufficient numbers of CD11b+ cells from the tumor directly, we purified CD11b+ cells from the spleen and exposed them to EPO *ex vivo*. As shown in Figure 5Bi, we detected an increase in STAT3-Tyr705 phosphorylation in these cells following 1 h of EPO exposure. Relative mRNA analysis of splenic CD11b+ cells that were stimulated with EPO for a day further showed an increased expression of two known STAT3 target genes, Bcl-3 and IL-23 (Figure 5Bii) (19,20). These findings implicate the potential role of CD11b+ myeloid cells and activation of the JAK/STAT3 signaling pathway, mediated via anemia-driven signals, in the acceleration of colon tumorigenesis observed in EPO-treated $APC^{Min/+}$ mice.

To validate the role of STAT3 activation in colon tumorigenesis, we treated fecal occult blood-positive $APC^{Min/+}$ mice with curcumin, a known STAT3 inhibitor (21). As curcumin has been demonstrated recently to decrease intestinal inflammation and tumor load in $APC^{Min/+}$ mice (22), we sought to establish if this effect in tumorigenesis is linked to STAT3 activation. Remarkably, we find that after 5 days of curcumin feeding, there was a significant reduction

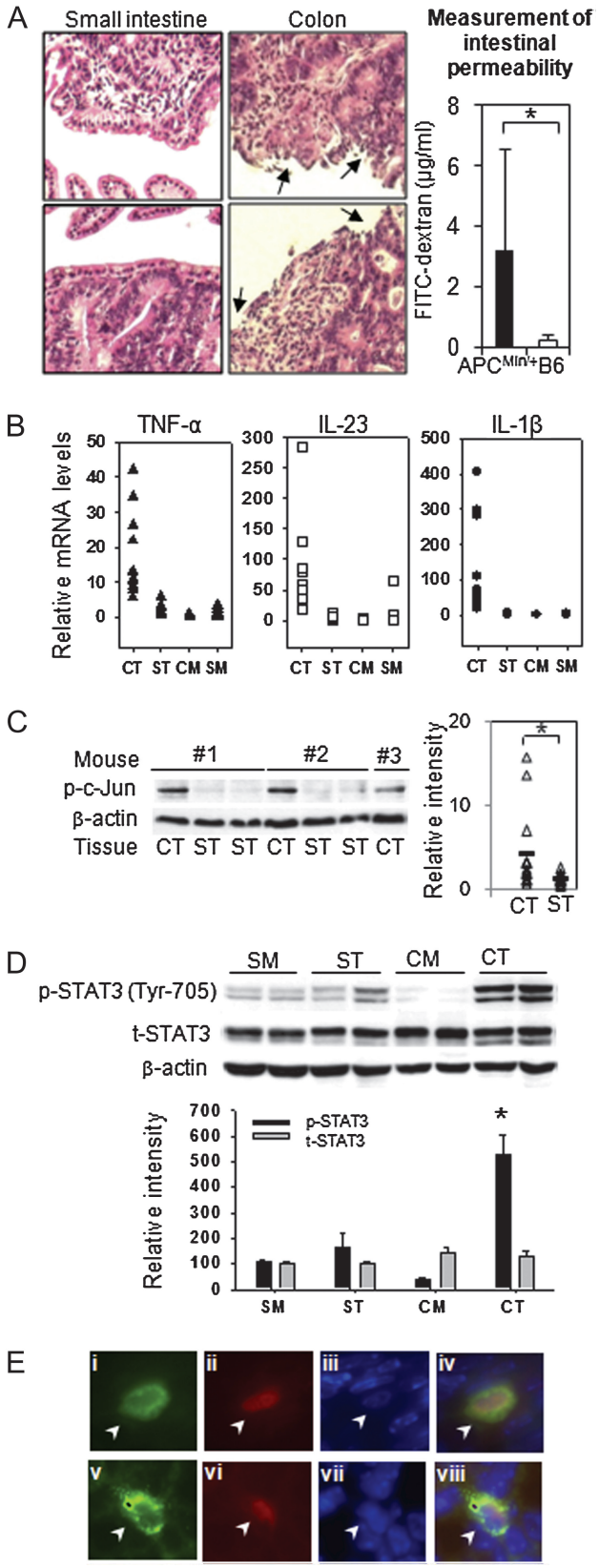

Fig. 2. Colonic but not small intestinal tumors display signs of inflammation. (**A**) Gut samples from 18- to 25-week-old SPF APC$^{Min/+}$ mice were fixed, sectioned and stained with hematoxylin and eosin. Picture represents cross-section of the adenomas in small intestine (left column) and colon (right column) at higher magnification. Intestinal gut barrier permeability was assessed via FITC-dextran assay (right plot). Concentration of FITC-dextran for each sample is presented as micrograms per milliliter. Asterisk indicates $P < 0.01$, Wilcoxon rank-sum test. (**B**) Colonic tumors in SPF APC$^{Min/+}$ mice express high levels of pro-inflammatory cytokines. Tumors were collected from 18- to 25-week-old APC$^{Min/+}$ mice and profiled for cytokine expression using quantitative real-time PCR. Relative expression levels of tumor necrosis factor (TNF)-α, IL-23 and IL-1β in tumors from colon ('CT') and small intestine ('ST') were compared with levels in normal mucosa of colon ('CM') and small intestine ('SM'). Analysis of variance applied to all groups showed significance level of $P < 0.05$ when CT was compared with both ST and CM groups for all three cytokine expression levels. (**C**) Colonic tumors in APC$^{Min/+}$ mice display higher levels of c-Jun phosphorylation than small intestinal tumors. Protein lysates of APC$^{Min/+}$ tumors from colon (CT) and small intestine (ST) were assayed for p-c-Jun as shown in a representative western blot (left panel). Relative quantification of p-c-Jun using densitometry, normalized with β-actin levels was performed for 14 CTs and 15 STs (right panel). Significance level of $P < 0.05$ (one-tailed *t*-test) between the CT and ST groups is indicated by an asterisk. (**D**) Colonic tumors in APC$^{Min/+}$ mice display elevated levels of tyrosine phosphorylated STAT3. Intestinal tumors (five CTs and five STs) and normal gut mucosal (four CMs and four SMs) samples were isolated from APC$^{Min/+}$ and age-matched B6 mice, respectively, lysed and analyzed by immunoblotting with p-STAT3 (Tyr-705) or STAT3 (t-STAT3) antibodies. Upper panel depicts a representative western blot, whereas lower panel represents relative densitometry quantification of p-STAT3 and t-STAT3 protein levels in pooled samples. An asterisk indicates a statistically significant difference in p-STAT3 levels of colonic tumors in comparison with all other groups ($P < 0.001$; analysis of variance). (**E**) CD11b+ myeloid cells in APC$^{Min/+}$ colonic tumors express high levels of p-STAT3 (Tyr-705) in nucleus. Upper and lower panels depict immunofluorescent staining of CD11b+ (green) (i and v), p-STAT3 (Tyr-705) (red) (ii and vi) and 4′,6-diamidino-2-phenylindole (blue) (iii and vii) in APC$^{Min/+}$ colonic tumors at ×100 magnification. Merged images (iv and viii) show nuclear colocalization of p-STAT3 in CD11b+ cells.

($P < 0.05$, *t*-test) in STAT3-Tyr705 phosphorylation in the colonic tumors of APC$^{Min/+}$ mice (Figure 5C). This finding thereby reaffirms the role of STAT3 activation in APC$^{Min/+}$ colon tumorigenesis.

LPS-dependent c-Jun phosphorylation promotes epithelial cell growth

We next examined whether factors secreted by activated CD11b+ myeloid cells can influence the c-Jun/JNK pathway since elevated levels of phosphorylated c-Jun were found in the colonic tumors. In our investigation, splenic CD11b+ cells were isolated from anemic, colon-tumor bearing APC$^{Min/+}$ mice and exposed to LPS, EPO or EPO and LPS for 24 h *ex vivo*. Conditioned media were collected and incubated with CT26 cells. As a control, CT26 cells were directly exposed to EPO or LPS. We found that conditioned medium from LPS-stimulated macrophages induced c-Jun phosphorylation in the epithelial cells (Figure 6A). Similarly, when primary colonic epithelial cells from GF B6 mice were exposed to LPS, an increase in c-Jun phosphorylation was observed (Figure 6C).

As c-Jun/JNK signaling has previously been reported to promote cell growth (23), we thus checked whether the increased c-Jun phosphorylation affected epithelial cell growth. To examine this, we measured the proliferation of CT26 cells following exposure to conditioned media from LPS, EPO or EPO and LPS stimulated myeloid cells, in the presence and absence of a c-Jun kinase inhibitor. As shown in Figure 6B, conditioned medium from LPS-stimulated CD11b+ cells accelerated CT26 cell proliferation, with an additive effect observed when cells were incubated with conditioned medium from LPS- and EPO-stimulated macrophages. This proliferative effect was diminished in the presence of JNK inhibitor II (JNKi), indicating that the promotion of cell growth was dependent on c-Jun phosphorylation (Figure 6B). As a negative control and to eliminate the possibility that the growth inhibition observed with JNKi was due to cytotoxic effects of the reagent, we measured cell viability via Trypan blue cell counting and did not find a significant reduction in cell viability with the use of JNKi (Supplementary Figure S10 is available at *Carcinogenesis* Online). Our data thus demonstrate that LPS-induced c-Jun phosphorylation and conditioned media from EPO stimulated myeloid cells can accelerate epithelial cell growth.

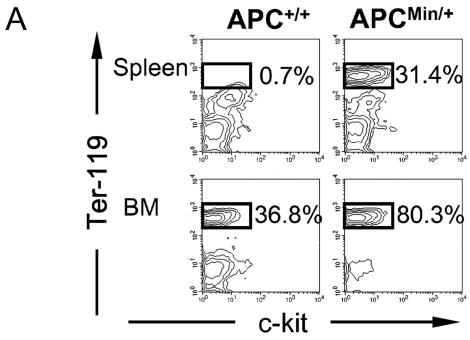

B

	APC$^{+/+}$	APC$^{Min/+}$
B lymphocytes (B220+)	44.3±3.9	80.9±27.3 *
T lymphocytes (CD4+)	19.4±3.9	24.4±9.0
T lymphocytes (CD8+)	11.8±2.5	12.3±4.0
NK cells (NK1.1+)	3.9±0.9	7.8±1.5 *
Myeloid cells (CD11b+ GR1-)	2.1±1.0	7.1±3.9
Myeloid cells (CD11b- GR1+)	6.3±1.6	13.3±3.7 *
Myeloid cells (CD11b+ GR1+)	0.9±0.5	4.5±1.4 *

Fig. 3. Reticulocyte counts are increased in spleen and bone marrow of aging APC$^{Min/+}$ mice. (**A**) Suspensions of bone marrow (BM) and lysed spleen cells were stained for erythroid-specific marker Ter-119 and c-kit. Flow cytometric analysis shows an expansion of erythroid cells (Ter-119+) in both BM and spleen. (**B**) Spleens of APC$^{Min/+}$ mice have increased counts of myeloid cells. Representative numbers ($\times 10^6$) of different splenic cell populations in spleens from 18- to 25-week-old APC$^{+/+}$ ($n = 5$) and APC$^{Min/+}$ ($n = 9$) mice, as measured by four-color FACS analysis using specific surface markers as indicated. Data are presented as means of fluorescence intensity ± standard deviation. Asterisk indicates $P < 0.05$, Wilcoxon rank-sum test.

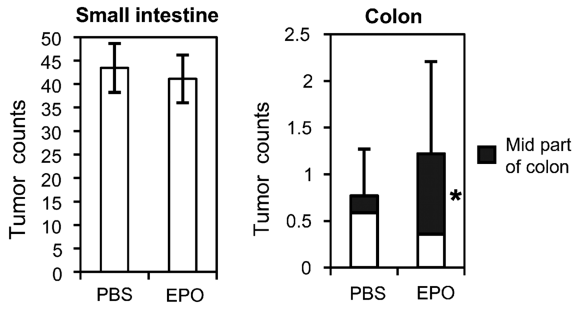

Fig. 4. Exposure to EPO leads to increased tumor counts in colon. APC$^{Min/+}$ mice were treated with either EPO or PBS for 7 days as described in Supplementary Figure S9A is available at *Carcinogenesis* Online. The figure summarizes tumor count in PBS treated ($n = 19$) or EPO treated ($n = 20$) mice, from three independently performed experiments. Tumor load in small intestine and colon is represented on the left and right panels, respectively. Error bars represent standard deviation. Significance level of $P < 0.05$ (Wilcoxon rank-sum test) between EPO and PBS group is indicated by an asterisk.

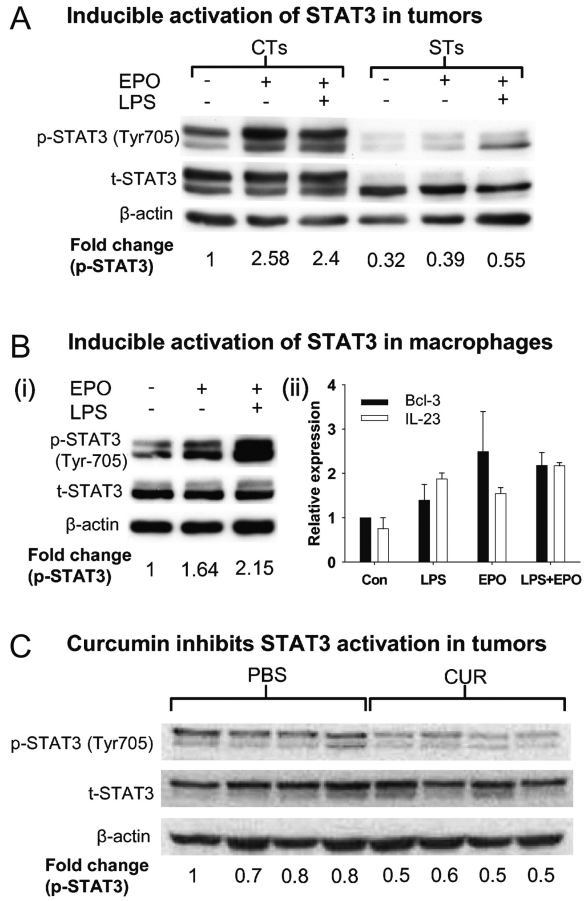

Fig. 5. EPO induces STAT3 tyrosine phosphorylation in APC$^{Min/+}$ colonic tumors and primary macrophages. Treatment of APC$^{Min/+}$ mice with curcumin inhibits STAT3 activation in colonic tumors. (**A**) Colonic tumors from APC$^{Min/+}$ mice were cultured *ex vivo* and either unstimulated (lane 1) or stimulated with medium containing EPO or EPO and LPS for 120 min and then analyzed for STAT3 phosphorylation (lanes 2 and 3, respectively). Intestinal tumors from APC$^{Min/+}$ mice were also collected and stimulated in parallel (lanes 4–6). Fold change values represent relative protein levels of p-STAT3 normalized with β-actin amounts by densitometry analysis. (**B**) (i) Purified splenic macrophages (CD11b+) from anemic APC$^{Min/+}$ mice were either unstimulated (lane 1) or stimulated with EPO or EPO and LPS (lanes 2 and 3, respectively) for 60 min and then assessed for p-STAT3 (Tyr-705) levels. (ii) Exposure of CD11b+ myeloid cells from APC$^{Min/+}$ mice to EPO, LPS or in combination *ex vivo* induces expression of IL23 (p19) and Bcl-3. Purified splenic CD11b+ cells were isolated from APC$^{Min/+}$ mice and cultured in RPMI-1640 medium only (Con) or medium containing LPS, EPO or LPS and EPO for 24 h. Cells were subsequently harvested for RNA extraction and analyzed for relative mRNA expression levels of STAT3 target genes, IL-23 and Bcl-3, as shown. Vertical axis represents relative fold change in gene expression, whereas error bars represent standard error mean. (C) APC$^{Min/+}$ mice with occult blood in feces were administered orally with curcumin or PBS for 5 days. Colonic tumors were then harvested and their whole cell extracts were analyzed for STAT3 phosphorylation.

Discussion

Here we identify two pathways, the c-Jun/JNK and STAT3 signaling pathways, which are triggered by microflora-originating signals and anemia, respectively, that act synergistically to enhance colonic tumor growth in APC$^{Min/+}$ mice. Our data suggests that microflora invasion into the lamina propria, following tumor-mediated disruption of the intestinal epithelial lining, may be more critical than previously perceived in initiating a 'vicious cycle' of anemia and inflammation leading to enhanced tumor growth through myeloid STAT3-dependent signals.

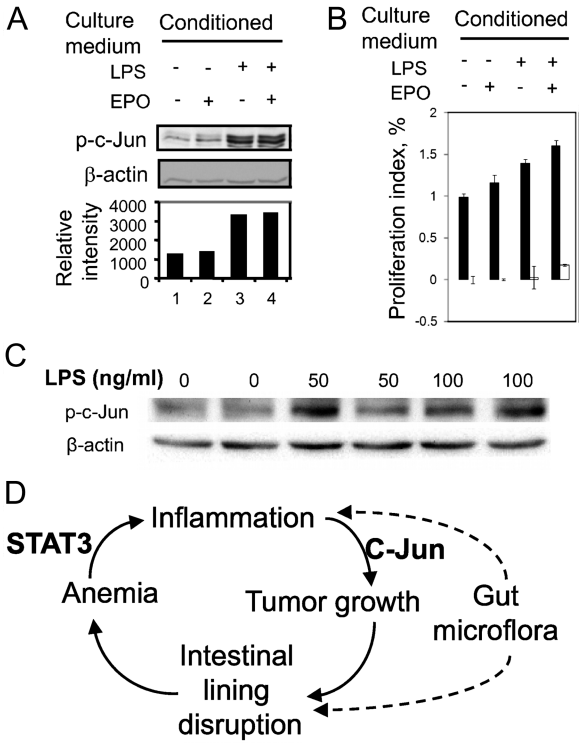

Fig. 6. Gut microbiota-derived LPS treatment stimulates c-Jun phosphorylation and proliferation of epithelial cells. (**A**) Cells of mouse carcinoma cell line CT26 were stimulated with medium conditioned with CD11b+ cells that were either unstimulated or stimulated with EPO, LPS or LPS and EPO for 24 h. The densitometry of phosphorylated c-Jun bands is presented with reference to β-actin control. Picture displays western blot of one representative experiment from three independent experiments with similar results. (**B**) Macrophage conditioned medium enhances LPS-induced proliferation of epithelial cells via c-Jun kinase dependent pathway. CT26 cells were starved for 24 h and then exposed to conditioned media of $APC^{Min/+}$ splenic macrophages that were treated for a day with LPS, EPO or LPS and EPO, in the presence and absence of JNK inhibitor II as indicated (white and black columns respectively). The MTS assay was performed on day 4 of the experiment. Values are depicted in relation to inhibitor-alone treated group. Error bars depict standard deviation. Picture displays one representative experiment from three independent experiments with similar results. (**C**) Primary colonic epithelial cells from GF B6 mice were stimulated with different LPS concentrations for 30 min and then subjected to western blot analysis of p-c-Jun (D) A proposed model of inflammation-driven tumorigenesis in $APC^{Min/+}$ mice, mediated by gut microbiota and anemia.

Gut microbiota has previously been suggested to be associated with regenerative epithelial cell growth as well as with tumor growth (4,24–26). This is further supported by the importance of a MyD88-dependent activation of NF-κB in myeloid cells for tumorigenesis in $APC^{Min/+}$ mice (12). Herein, we provide two lines of evidence that reinforce the critical role of gut microflora and myeloid-dependent inflammation in accelerating colonic tumor growth, namely that (i) GF $APC^{Min/+}$ mice are virtually devoid of colonic tumors (Figure 1) and (ii) macrophage-specific deletion of IκB kinase β abrogate colonic tumors in SPF $APC^{Min/+}$ mice (Supplementary Figure S5 is available at *Carcinogenesis* Online).

The analysis of GF $APC^{Min/+}$ mice has previously been investigated by Dove *et al.* (27). Although our tumor counts for GF $APC^{Min/+}$ mice are similar to their study, we find that contrary to their conclusions whereby no significant difference in total intestinal tumor load between GF mice and conventional controls was found and thus independence of tumorigenesis from microbial status, our SPF $APC^{Min/+}$ mice developed significantly more intestinal tumors. These distinct observations highlight the potential impact of different animal housing conditions and environment on microflora composition and diversity in the $APC^{Min/+}$ mice and thus tumor load. This is an interesting proposition that needs further investigation that is not within the scope of our present study.

In our characterization of the intestinal tumors of SPF $APC^{Min/+}$ mice, we observe a distinct inflammatory status in colonic tumors, relative to small intestinal tumors and normal mucosa tissues. Notably, we detect elevated mRNA levels of IL-23, a pro-inflammatory cytokine which has been reported to be an important factor in tumorigenesis and is induced by enterotoxins from *Bacteroides fragilis* (26), in our $APC^{Min/+}$ colonic tumors. Moreover, our *ex vivo* macrophage stimulation assays show an induction of IL-23 mRNA expression following exposure to LPS and EPO, which correlates with increased STAT3 phosphorylation (Figure 5Bii). These findings thus lead us to speculate that the innate immune MyD88-dependent NF-κB signaling pathway (triggered by gut microbiotal components), as well as anemia-mediated signals, can induce IL-23 in myeloid cells through activation of STAT3.

A major inflammation-related culprit of pathogenesis in $APC^{Min/+}$ mice with advanced intestinal and particularly, colonic tumors is intestinal bleeding, which induces anemia and concomitant erythropoiesis (7). EPO is a hormone that is known to stimulate erythropoiesis and activate myeloid cells (17) and in an attempt to mimic the anemic signaling pathway in non-anemic $APC^{Min/+}$ mice, we treated them with EPO. Our findings show that administration of EPO *in vivo* accelerates colonic tumor growth in non-anemic $APC^{Min/+}$ mice (Figure 4). In contrast, the lack of EPO effect on the tumor load of GF $APC^{Min/+}$ mice suggests that anemia-driven factors interact with signals from the gut microbiome to accelerate tumor growth. In our *ex vivo* culture assays using $APC^{Min/+}$ colonic tumors and purified CD11b+ myeloid cells, an increased phosphorylation of STAT3 with EPO exposure in both colonic tumors and myeloid cells was detected (Figure 5A and B). Additional analysis of these cells revealed an increased expression of two STAT3 responsive genes, Bcl-3 and IL-23 (Figure 5Bii). Interestingly, Bcl-3 and IL-23 have been linked to apoptotic resistance and inflammation, respectively, trademarks of tumor promotion (3,28). Notably, oral administration of $APC^{Min/+}$ mice with curcumin, a chemical known to reduce intestinal tumorigenesis in these mice, decreased STAT3 phosphorylation in colonic tumors, thus linking STAT3 activation with colonic tumor growth. Hence, while our results are in line with previous work on myeloid cells and tumor progression (29,30), they also highlight the role of anemia in promoting tumor growth via the JAK/STAT3 signaling pathway.

Earlier work by several groups have identified elevated levels of tyrosine-phosphorylated STAT3 as a negative prognostic factor for various cancers including CRC (10), propelling STAT3 as a major molecular bridge between chronic inflammation and tumorigenesis. However, while STAT3 has been shown to have pro-proliferative effects in the initial stages of tumor growth, its expression in intestinal epithelial cells has been suggested in a recent study to inhibit tumor progression at later stages (31). In another recent study, the genetic ablation of STAT3 in macrophages (and also partially in other hematopoietic cells) was linked to the development of colonic tumors (32). However, the tumor incidence reported was extremely low and the genetic ablation affected various hematopoietic cell lineages, which may cause defects in hematopoietic differentiation that are cancer promoting. Thus, the correlation of STAT3 activation with respect to the prognosis of cancers needs to be interpreted with caution. Intriguingly, the presence of high levels of nuclear p-STAT3 (Tyr-705) that we detect in the myeloid cells associated with $APC^{Min/+}$ colonic tumors (Figure 2E; Supplementary Figure S7 is available at *Carcinogenesis* Online), as well as the EPO effects that we observe, suggest the ability of STAT3 to cooperate with NF-κB in myeloid cells to promote colonic tumor growth in these mice. Our findings are also in line with previous reports demonstrating alternative roles for EPO besides erythropoiesis, such as regeneration of myocardia in ischemic tissue and EPO-induced STAT3 activation in myeloid cells (33).

There appears to be a discrepancy in EPO effect on tumor cell lines and *in vivo* cancer models whereby EPO did not exert proliferative effects *in vitro* but promotes tumor growth and

angiogenesis in mouse tumor models (34,35). This is probably due to EPO exerting its tumor-promoting effects on bystander cells in the tumor microenvironment, as suggested by our data. While EPO initially was used as a vehicle to mimic anemia-induced signaling pathways in $APC^{Min/+}$ mice, our data disclose a potentially harmful effect of EPO. This raises some concerns about the use of EPO under anemic conditions in patients with high tumor load. Indeed, the Breast Cancer Erythropoietin Trial (BEST) (36) and the Amgen 20010103 clinical trial (Amgen 103) (37), both reported that EPO treatment was associated with a higher mortality rate. Our data may in part explain some of these unwanted effects.

While tumorigenesis in $APC^{Min/+}$ mice is known to depend on an active Wnt/β-catenin pathway, additional tumor-promoting signals have been reported (25,38,39). One such accessory signal is the phosphorylation and activation of c-Jun a member of the AP-1 transcription complex (9). Here we show that c-Jun phosphorylation in epithelial cells can be induced by LPS alone or in combination with factors secreted by CD11b+ myeloid cells and stimulate cell proliferation in a JNK-dependent manner (Figure 6A–C). Thus, our results support an AP-1 driven tumor-promoting mechanism, acting in addition and distinct from the Wnt/β-catenin pathway (40).

Major health problems such as cardiovascular diseases (41), Crohn's disease (42) and various cancers (43–45) have recently been reported to have host-microbe connections. Yet we are only beginning to understand the molecular mechanisms underlying the link between microbes, chronic inflammation and disease development. Our data should therefore be viewed as an initial attempt to mechanistically explain how gut microflora can fuel a vicious cycle of epithelial lining disruption that accelerates inflammation and anemia and ultimately tumor growth (Figure 6D). Further studies utilizing STAT3 and c-Jun mediated signaling pathways in myeloid and tumor cells, respectively, in other inflammation driven tumor models outside the intestinal tract is therefore highly warranted.

Supplementary material

Supplementary Figures 1–11 can be found at http://carcin.oxfordjournals.org/

Funding

Swedish Foundation for Strategic Research (SSF) to S.P. and K.K.; Swedish foundation for Cancer Research (Cancerfonden) and Singapore National Cancer Centre Research Fund (NCCRF) to S.P.; Singapore Millenium Foundation, Singapore to S.P. and G.G. A*STAR scholarship to Y.L.

Acknowledgements

We thank Drs J. Rafter, V.Arulampalam, S.Pott, M.Frericks and P.Reilly for critical reading and Low Meijun, Teo Weiling and Annika Samuelsson for technical assistance. The help from staff at the core facility for germ free research at KI is also acknowledged.

Conflict of Interest Statement: None declared.

References

1. Grivennikov,S.I. *et al*. (2010) Immunity, inflammation, and cancer. *Cell*, **140**, 883–899.
2. Atreya,R. *et al*. (2008) Signaling molecules: the pathogenic role of the IL-6/STAT-3 trans signaling pathway in intestinal inflammation and in colonic cancer. *Curr. Drug Targets*, **9**, 369–374.
3. Langowski,J.L. *et al*. (2006) IL-23 promotes tumour incidence and growth. *Nature*, **442**, 461–465.
4. Greten,F.R. *et al*. (2004) IKKbeta links inflammation and tumorigenesis in a mouse model of colitis-associated cancer. *Cell*, **118**, 285–296.
5. Ewaschuk,J.B. *et al*. (2006) The role of antibiotic and probiotic therapies in current and future management of inflammatory bowel disease. *Curr. Gastroenterol. Rep.*, **8**, 486–498.
6. Elson,C.O. *et al*. (2005) Experimental models of inflammatory bowel disease reveal innate, adaptive, and regulatory mechanisms of host dialogue with the microbiota. *Immunol. Rev.*, **206**, 260–276.
7. Moser,A.R. *et al*. (1990) A dominant mutation that predisposes to multiple intestinal neoplasia in the mouse. *Science*, **247**, 322–324.
8. Gregorieff,A. *et al*. (2005) Wnt signaling in the intestinal epithelium: from endoderm to cancer. *Genes Dev.*, **19**, 877–890.
9. Nateri,A.S. *et al*. (2005) Interaction of phosphorylated c-Jun with TCF4 regulates intestinal cancer development. *Nature*, **437**, 281–285.
10. Kusaba,T. *et al*. (2006) Activation of STAT3 is a marker of poor prognosis in human colorectal cancer. *Oncol. Rep.*, **15**, 1445–1451.
11. Desai,J. *et al*. (2005) Recombinant human erythropoietin in cancer-related anemia: an evidence-based review. *Best Pract. Res. Clin. Haematol.*, **18**, 389–406.
12. Rakoff-Nahoum,S. *et al*. (2007) Regulation of spontaneous intestinal tumorigenesis through the adaptor protein MyD88. *Science*, **317**, 124–127.
13. Pull,S.L. *et al*. (2005) Activated macrophages are an adaptive element of the colonic epithelial progenitor niche necessary for regenerative responses to injury. *Proc. Natl Acad. Sci. USA*, **102**, 99–104.
14. Schuringa,J.-J. *et al*. (2001) c-Jun and c-Fos cooperate with STAT3 in IL-6-induced transactivation of the IL-6 response element (IRE). *Cytokine*, **14**, 78–87.
15. Knight,K. *et al*. (2004) Prevalence and outcomes of anemia in cancer: a systematic review of the literature. *Am. J. Med.*, **116**, 11–26.
16. Half,E. *et al*. (2009) Familial adenomatous polyposis. *Orphanet J. Rare Dis.*, **4**, 22.
17. Koya,T. *et al*. (1999) Erythropoietin induces the expansion of c-kit+ progenitors for myeloid and erythroid cells, but not for lymphoid cells, in the bone marrow and liver. *Eur. J. Haematol.*, **63**, 306–312.
18. Wierenga,A.T. *et al*. (2003) Erythropoietin-induced serine 727 phosphorylation of STAT3 in erythroid cells is mediated by a MEK-, ERK-, and MSK1-dependent pathway. *Exp. Hematol.*, **31**, 398–405.
19. Brocke-Heidrich,K. *et al*. (2006) BCL3 is induced by IL-6 via Stat3 binding to intronic enhancer HS4 and represses its own transcription. *Oncogene*, **25**, 7297–7304.
20. Kortylewski,M. *et al*. (2010) Regulation of the IL-23 and IL-12 balance by Stat3 signaling in the tumor microenvironment. *Cancer Cell*, **15**, 114–123.
21. Uddin,S. *et al*. (2005) Curcumin suppresses growth and induces apoptosis in primary effusion lymphoma. *Oncogene*, **24**, 7022–7030.
22. Murphy,E.A. *et al*. (2011) Curcumin's effect on intestinal inflammation and tumorigenesis in the ApcMin/+ mouse. *J. Interferon Cytokine Res.*, **31**, 219–226.
23. Sancho,R. *et al*. (2009) JNK signalling modulates intestinal homeostasis and tumourigenesis in mice. *EMBO J.*, **28**, 1843–1854.
24. Oguma,K. *et al*. (2008) Activated macrophages promote Wnt signalling through tumour necrosis factor-alpha in gastric tumour cells. *EMBO J.*, **27**, 1671–1681.
25. Newman,J.V. *et al*. (2001) Bacterial infection promotes colon tumorigenesis in Apc(Min/+) mice. *J. Infect. Dis.*, **184**, 227–230.
26. Wu,S. *et al*. (2009) A human colonic commensal promotes colon tumorigenesis via activation of T helper type 17 T cell responses. *Nat. Med.*, **15**, 1016–1022.
27. Dove,W.F. *et al*. (1997) Intestinal neoplasia in the ApcMin mouse: independence from the microbial and natural killer (beige Locus) status. *Cancer Res.*, **57**, 812–814.
28. Choi,H.J. *et al*. (2010) Bcl3-dependent stabilization of CtBP1 is crucial for the inhibition of apoptosis and tumor progression in breast cancer. *Biochem. Biophys. Res. Commun.*, **400**, 396–402.
29. Bunt,S.K. *et al*. (2006) Inflammation induces myeloid-derived suppressor cells that facilitate tumor progression. *J. Immunol.*, **176**, 284–290.
30. Serafini,P. *et al*. (2004) Derangement of immune responses by myeloid suppressor cells. *Cancer Immunol. Immunother.*, **53**, 64–72.
31. Musteanu,M. *et al*. (2009) Stat3 is a negative regulator of intestinal tumor progression in ApcMin mice. *Gastroenterology*, **138**, 1003–1011.
32. Deng,L. *et al*. (2010) A novel mouse model of inflammatory bowel disease links mammalian target of rapamycin-dependent hyperproliferation of colonic epithelium to inflammation-associated tumorigenesis. *Am. J. Pathol.*, **176**, 952–967.
33. Lifshitz,L. *et al*. (2009) Non-erythroid activities of erythropoietin: functional effects on murine dendritic cells. *Mol. Immunol.*, **46**, 713–721.
34. Hardee,M.E. *et al*. (2005) Human recombinant erythropoietin (rEpo) has no effect on tumour growth or angiogenesis. *Br. J. Cancer*, **93**, 1350–1355.

35. Xue,Y. *et al*. (2011) PDGF-BB modulates hematopoiesis and tumor angiogenesis by inducing erythropoietin production in stromal cells. *Nat. Med.*, **18**, 100–110.
36. Leyland-Jones,B. *et al*. (2005) Maintaining normal hemoglobin levels with epoetin alfa in mainly nonanemic patients with metastatic breast cancer receiving first-line chemotherapy: a survival study. *J. Clin. Oncol.*, **23**, 5960–5972.
37. Smith,R.E.Jr *et al*. (2008) Darbepoetin alpha for the treatment of anemia in patients with active cancer not receiving chemotherapy or radiotherapy: results of a phase III, multicenter, randomized, double-blind, placebo-controlled study. *J. Clin. Oncol.*, **26**, 1040–1050.
38. Phelps,R.A. *et al*. (2009) A two-step model for colon adenoma initiation and progression caused by APC loss. *Cell*, **137**, 623–634.
39. Wang,T. *et al*. (2007) Notch3 activation modulates cell growth behaviour and cross-talk to Wnt/TCF signalling pathway. *Cell. Signal.*, **19**, 2458–2467.
40. Nordling,M.M. *et al*. (2003) Effects on cell proliferation, activator protein-1 and genotoxicity by fecal water from patients with colorectal adenomas. *Scand. J. Gastroenterol.*, **38**, 549–555.
41. Wang,Z. *et al*. (2011) Gut flora metabolism of phosphatidylcholine promotes cardiovascular disease. *Nature*, **472**, 57–63.
42. Sokol,H. *et al*. (2006) Specificities of the fecal microbiota in inflammatory bowel disease. *Inflamm. Bowel Dis.*, **12**, 106–111.
43. Correa,P. *et al*. (2007) Carcinogenesis of *Helicobacter pylori*. *Gastroenterology*, **133**, 659–672.
44. Rao,V.P. *et al*. (2006) Innate immune inflammatory response against enteric bacteria *Helicobacter hepaticus* induces mammary adenocarcinoma in mice. *Cancer Res.*, **66**, 7395–7400.
45. Nagamine,C.M. *et al*. (2008) *Helicobacter hepaticus* infection promotes colon tumorigenesis in the BALB/c-Rag2(-/-) Apc(Min/+) mouse. *Infect. Immun.*, **76**, 2758–2766.

Received June 8, 2011; revised March 18, 2012; accepted March 23, 2012